

A Novel Measure to Evaluate Generative Adversarial Networks Based on Direct Analysis of Generated Images

Shuyue Guan, Murray Loew

Department of Biomedical Engineering, the George Washington University, Washington DC, USA
{frankshuyueguan, loew}@gwu.edu

Abstract

The Generative Adversarial Network (GAN) is a state-of-the-art technique in the field of deep learning. A number of recent papers address the theory and applications of GANs in various fields of image processing. Fewer studies, however, have directly evaluated GAN outputs. Those that have been conducted focused on using classification performance (e.g., Inception Score) and statistical metrics (e.g., Fréchet Inception Distance). Here, we consider a fundamental way to evaluate GANs by directly analyzing the images they generate, instead of using them as inputs to other classifiers. We characterize the performance of a GAN as an image generator according to three aspects: 1) Creativity: non-duplication of the real images. 2) Inheritance: generated images should have the same style, which retains key features of the real images. 3) Diversity: generated images are different from each other. A GAN should not generate a few different images repeatedly. Based on the three aspects of ideal GANs, we have designed the Likeness Score (LS) to evaluate GAN performance, and have applied it to evaluate several typical GANs. We compared our proposed measure with three commonly used GAN evaluation methods: Inception Score (IS), Fréchet Inception Distance (FID) and 1-Nearest Neighbor classifier (1NNC). In addition, we discuss how these evaluations could help us deepen our understanding of GANs and improve their performance.

1. Introduction

As neural-network based generators, Generative Adversarial Networks (GANs) were introduced by Goodfellow *et al.* in 2014 [1], and they have become a state-of-the-art technique in the field of deep learning [2]. Recently, the number of types of GANs has grown to about 500 [3] and a substantial number of studies are about the theory and applications of GANs in various fields of image processing, including image translation [4], [5], object detection [6], super-resolution [7], image synthesis [8] and image blending [9]. Compared to the theoretical progress and applications of GANs, fewer studies have focused on evaluating or measuring GANs' performance [10]. Most existing GANs' measures have been conducted using classification performance (e.g., Inception Score) and statistical metrics (e.g., Fréchet Inception Distance). Alternatively, a more fundamental approach to evaluate a GAN is to directly analyze the images it generated, instead

of using them as inputs to other classifiers (e.g. Inception Network) and then analyzing the outcomes.

In this study, we try to establish a fundamental way to analyze GAN-generated images quantitatively and qualitatively. We briefly summarize three commonly used GAN evaluation methods: Inception Score (IS) [11], Fréchet Inception Distance (FID) [12], and 1-Nearest Neighbor classifier (1NNC) [13], and compared those results with our proposed measure. In addition, we discussed how these evaluations could help us to deepen our understanding of GANs and to improve their performance.

1.1. GAN Evaluation Metrics

The optimal GAN for images can generate images that have the same distribution as real samples (used for training), are different from real ones (not duplication), and have variety. Expectations of generated images could be described by three aspects: 1) non-duplication of the real images, 2) generated images should have the same style, which we take to mean that their distribution is close to that of the real images, and 3) generated images are different from each other. Therefore, we evaluate the performance of a GAN as an image generator according to **the three aspects**:

- **Creativity**: non-duplication of the real images. It checks for overfitting by GANs.
- **Inheritance**: generated images should have the same style, which retains key features of the real (input) images. And this is traded off with the creativity property because generated images should not be too similar nor too dissimilar to the real ones.
- **Diversity**: generated images are different from each other. A GAN should not generate a few dissimilar images repeatedly.

Fig. 1 displays four counterexamples of ideal generated images.

We introduce a distance-based separability index and use it to define the measure: Likeness Score (LS) to evaluate GAN performance according to the three expectations of ideal generated images. LS offers a direct way to measure difference or similarity between images based on the Euclidean distance and has a simple and uniform framework for the three aspects of ideal GANs and depends less on visual evaluation.

The proposed LS measure is applied to analyze the generated images directly, without using pre-trained

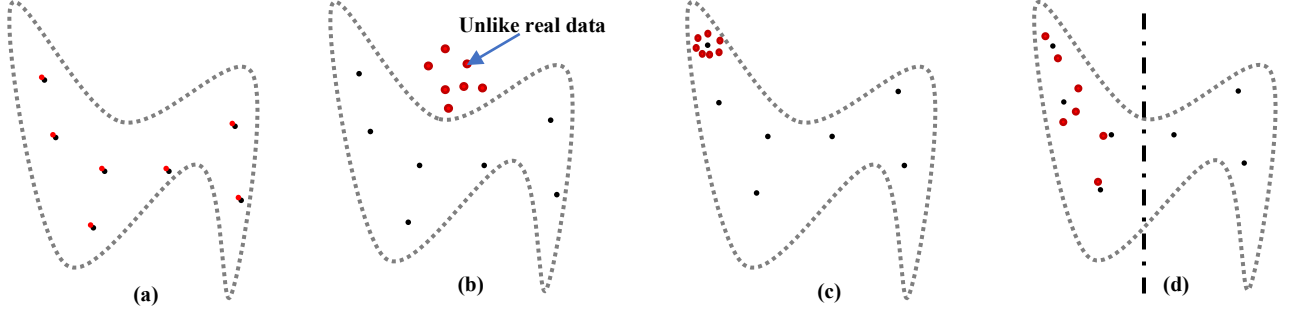


Fig. 1 Problems of generated images from the perspective of distribution. The area of dotted line is the distribution of real images. The dark-blue dots are real samples and red dots are generated images. (a) is overfitting, lack of Creativity. (b) is lack of Inheritance. (c) is called mode collapse for GAN and (d) is mode dropping. Both (c) and (d) are examples of lack of Diversity.

classifiers. We applied the measure to outcomes of several typical GANs: DCGAN [14], WGAN-GP [15], SNGAN [16] LSGAN [17] and SAGAN [18] on various image datasets. Results show that the LS can reflect the performance of GAN well and are very competitive with other compared measures. In addition, the LS is stable with respect to the number of images and could provide explanation of results in terms of the three respects of ideal GANs.

1.2. Related Work

The **Inception Score (IS)** [11] is a commonly applied index to evaluate GANs' performance. To compute the IS, we submit generated images to the Inception network [19] that was pre-trained on the ImageNet [20] dataset. From the perspective of the three aspects for ideal GANs, the IS focuses on measuring the inheritance and diversity. Specifically, we let $x \in G$ be a generated image; $y = \text{InceptionNet}(x)$ is the label obtained from the pre-trained Inception network by inputting image x . For all generated images, we have the label set Y . $H(Y)$ defines the diversity ($H(\cdot)$ is entropy) because the variability of labels reflects the variability of images. $H(Y|G)$ could show the inheritance because a good generated image can be well recognized and classified, and thus the entropy of $p(y|x)$ should be small. Therefore, an ideal GAN will maximize $H(Y)$ and minimize $H(Y|G)$. Equivalently, the goal is to maximize:

$$\begin{aligned} & H(Y) - H(Y|G) \\ &= -\sum_y p(y) \log p(y) - \sum_x p(x) H(y|x) \\ &= \sum_y p(y) \log \frac{1}{p(y)} + \sum_x \sum_y p(x) p(y|x) \log p(y|x) \end{aligned}$$

Since $\sum_x p(x) = 1$

$$\begin{aligned} &= \sum_x \sum_y \left[p(x) p(y|x) \log \frac{1}{p(y)} + p(x) p(y|x) \log p(y|x) \right] \\ &= \sum_x p(x) \sum_y p(y|x) \log \frac{p(y|x)}{p(y)} \end{aligned}$$

$$= \sum_x p(x) \mathbf{D}_{KL}[p(y|x)||p(y)] = \mathbf{E}_G[\mathbf{D}_{KL}(p(y|x)||p(y))]$$

\mathbf{D}_{KL} is the Kullback–Leibler (KL) divergence of two distributions [21]. The IS index is defined:

$$IS(G) = \exp(\mathbf{E}_G[\mathbf{D}_{KL}(p(y|x)||p(y))])$$

The IS mainly shows diversity and reflects inheritance to some extent; a larger value of IS indicates that a GAN's performance is better. The substantial limitations of IS are: 1) it **depends on classification of images by the Inception network**, which is by trained ImageNet, and employs generated data **without exploiting real data**. Thus, IS may not be proper to use on other images or non-classification tasks because it cannot properly show the inheritance if the data are different from those used in ImageNet. 2) Since **creativity is not considered by the IS**, it has no ability to detect overfitting. For example, if generated images set was a copy of real images and very similar to images of ImageNet, IS will give a high score.

Fréchet Inception Distance (FID) [12] exploits real data and also uses the pre-trained Inception network. Instead of output labels it uses feature vectors from the final pooling layers of InceptionNet. All real and generated images are input to the network to extract their feature vectors.

Let $\varphi(\cdot) = \text{InceptionNet_lastPooling}(\cdot)$ be the feature extractor and let $F_r = \varphi(R), F_g = \varphi(G)$ be two groups of feature vectors extracted from real and generated image sets. Consider that the distributions of F_r, F_g are multivariate Gaussian:

$$F_r \sim N(\mu_r, \Sigma_r); F_g \sim N(\mu_g, \Sigma_g)$$

The difference of two Gaussians is measured by the Fréchet distance:

$$FID(R, G) = \|\mu_r - \mu_g\|_2^2 + \text{Tr}(\Sigma_r + \Sigma_g - 2(\Sigma_r \Sigma_g)^{1/2})$$

In fact, FID measures the difference between distributions of real and generated images; that agrees with the goal of GAN training – to minimize the difference between the two distributions. But the **Gaussian distribution assumption** of

feature vectors cannot be guaranteed. And, as with IS, it depends on the pre-trained Inception network.

The measure: **1-Nearest Neighbor classifier (1NNC)** [13] does not require an additional classifier. Instead, it uses a two-sample test with the 1-Nearest Neighbor method on real and generated image sets. Similar to FID, 1NNC examines whether two distributions of real and generated image are identical, but it requires the numbers of real and generated images to be equal.

Suppose $|R| = |G|$, and we wish to compute the leave-one-out (LOO) accuracy of a 1-NN classifier trained on R and G with labels “1” for R and “0” for G . In the optimal situation, the LOO accuracy ≈ 0.5 because the two distributions are very similar. If LOO accuracy < 0.5 , the GAN is overfitting to R because the generated data are very close to the real samples. In an extreme case, if the GAN memorizes every sample in R and then generates them identically, i.e., $G = R$, the accuracy would be 0 because every sample from R would have its nearest neighbor from G with zero distance. LOO accuracy > 0.5 means the two distributions are different (separable). If they are completely separable, the accuracy would be 1.0.

Compared to IS and FID, 1NNC seems a more independent measure. However, the $|R| = |G|$ requirement limits its applications and **the local conditions of distributions** will greatly affect the 1-NN classifier. For IS, higher values imply better performance of GANs; and for FID, lower is better. But for 1NNC, 0.5 is the best score. We regularize 1NNC by this function:

$$r(x) = -|2x - 1| + 1$$

$r1NNC = r(1NNC)$. For $r1NNC$, the best score is 1.

2. Likeness Score

Because the FID and 1NNC are effective ways to examine how the distributions of real and generated images are close to each other, they are also an effective way to measure GANs because the goal of GAN training is to make generated images have the same distribution as real ones. Consider a two-class dataset in which real data and generated data sets are defined by the maximum entropy principle (MEP); this is the most difficult situation for separation of the data because the two classes of data are **scattered and mixed together in the same distribution**. In this sense, the **separability** of real and generated data could be a promising measure of the similarity of the two distributions. As the separability increases, the two distributions have more differences.

Based on the MEP, we could define the data separability as being inversely related to the system’s entropy. To

calculate the entropy, we divide the space into many small regions. Then, the proportions of each class in every small region can be considered as their occurrence probabilities. The system’s entropy can be derived from those probabilities. In high-dimensional spaces for images, however, the number of small regions grows exponentially. For example, for 32x32 pixels 8-bit RGB images, the space has 3,072 dimensions. If each dimension (the range is from 0 to 255) is divided to 32 intervals, the total number of small regions is $32^{3072} \approx 6.62 \times 10^{4623}$. It is impossible to compute the system’s entropy in this way.

Alternatively, we propose the **Distance-based Separability Index (DSI)** as a substitute of entropy to analyze how the two classes of data are mixed together. Consider two classes X, Y that have the same distribution covering the same region and have sufficient points. Suppose X, Y have N_x, N_y points respectively, we define that the **Intra-Class distance (ICD) set** is the set of distances between any two points in the same class (X):

$$\{d_x\} = \{\|x_i - x_j\|_2 | x_i, x_j \in X; x_i \neq x_j\}$$

$$\text{If } |X| = N_x, \text{ then } |\{d_x\}| = \frac{1}{2} N_x (N_x - 1).$$

And the **Between-class distance (BCD) set** is the set of distances between any two points from different classes (X, Y):

$$\{d_{x,y}\} = \{\|x_i - y_j\|_2 | x_i \in X; y_j \in Y\}$$

$$\text{If } |X| = N_x, |Y| = N_y, \text{ then } |\{d_{x,y}\}| = N_x N_y.$$

It can be proven¹ that: if and only if two classes X, Y have the same distribution covering the same region and have sufficient points, the distributions of ICD and BCD sets are nearly identical. Hence, if the distributions of the ICD and BCD sets are nearly identical, the system has the maximum entropy and thus has the worst separability. The metric of distance is Euclidean (l^2 -norm). The time cost for ICD and BCD sets is linear with dimension and quadratic with the number of observations. It is much better than computing the system’s entropy by dividing the space into many small regions.

2.1. Computation of DSI

First, we compute the ICD sets of real image set R and generated image set G : $\{d_r\}, \{d_g\}$ and the BCD set: $\{d_{r,g}\}$. To examine the similarity of the distributions of ICD and BCD sets, we apply the Kolmogorov–Smirnov test (K-S test) [22]. Although there are many statistical measures to

¹ We do not show the proof here because it is detailed and not relevant to the main topic. It will appear in another forthcoming publication. Since the statement is intuitive, we provide an informal explanation here: points in X, Y having the same distribution and covering the same region can be considered to have been sampled from one distribution Z . Hence, both ICDs of X, Y and BCDs between X, Y are **actually ICDs of Z** . Consequently, the distributions of ICDs and BCDs are identical.

compare two distributions, such as Bhattacharyya distance, Kullback–Leibler divergence, and Jensen–Shannon divergence, most of them require that the two sets have the same number of observations. It is easy to show that the $\{|d_r\}$, $\{|d_g\}$ and $\{|d_{r,g}\}$ cannot be the same length. Then, we compute the similarities between ICD sets and BCD sets by the K-S test: $s_r = KS(\{|d_r\}, \{|d_{r,g}\})$, $s_g = KS(\{|d_g\}, \{|d_{r,g}\})$. The DSI is the maximum of two KS similarities: $DSI(\{R, G\}) = \max\{s_r, s_g\}$ because the maximum value can highlight the difference between ICD and BCD sets. $KS(\{|d_r\}, \{|d_g\})$ is not considered because it shows only the difference of distribution shapes, not including their location information. For example, two distributions that have the same shape, but no overlap will have similarities between ICD: $KS(\{|d_1\}, \{|d_2\})$ equal to zero.

2.2. DSI and GAN Evaluation

Fig. 2 displays artificial 2D examples of generated data (orange points; blue points are real data) that respectively lack creativity, diversity, and inheritance. With respect to the ICD and BCD sets, if the generated data overfit the real data (lack of creativity), peaks will appear in the distribution of BCD near zero (see Fig. 2a) because there are many generated points that are close to real data points in their distribution space; hence, many BCD are close to zero. Similarly, lack of diversity implies that many generated data points are close to each other; thus many ICD are close to zero and peaks will appear in the distribution of ICD near zero (see Fig. 2b). Lack of inheritance is shown by the difference between the distribution of ICD and BCD (see Fig. 2c) because if and only if two classes (real data and generated data) have the same distribution (shapes) covering the same region, the distributions of ICD and BCD sets are identical. In that case, there is neither lack of creativity nor lack of diversity. This is because there will be **no single peaks of ICD or BCD near zero**. Therefore, the DSI well evaluates the GAN’s performance by measuring creativity, diversity, and inheritance. DSI ranges from 0 to 1; DSI is close to 1 when the distributions of real and generated data are more different. To be consistent with other comparison measures, we complement its value and define the **Likeness Score (LS)** $= 1 - DSI$, which is closer to 1 if the GAN performs better.

3. Experiments & Results

The first experiment has two purposes: one is to test the stability of the proposed measure, *i.e.*, how little the results change when different amounts of data are used. Another purpose is to find the minimum amount of data required for the following experiments because a GAN could generate unlimited data and we wish to bound it to make computation practicable.

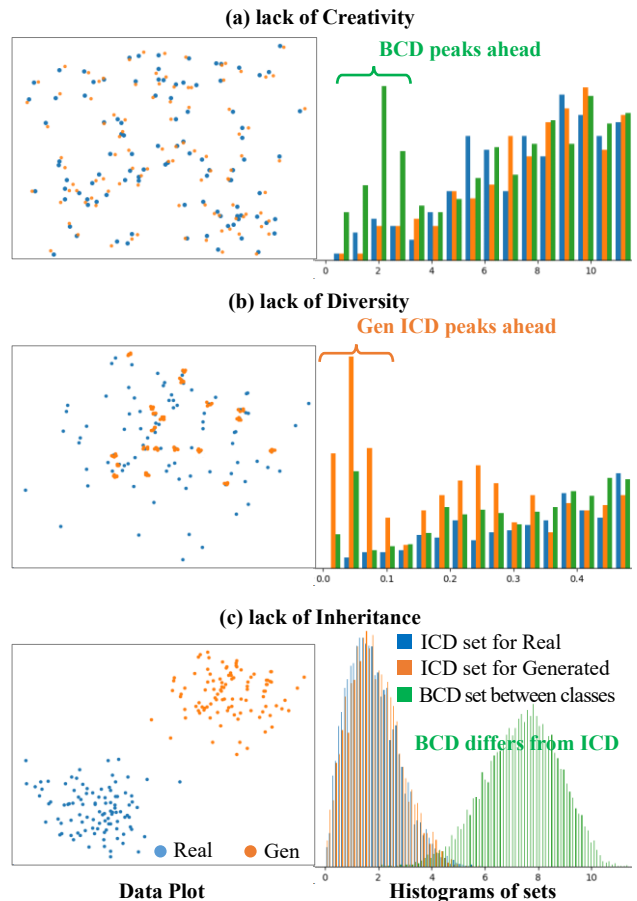


Fig. 2. Lack of Creativity, Diversity, and Inheritance in 2D. Histograms of (a) and (b) are zoomed to ranges near zero; (c) has the entire histogram.

The following experiments are to compare our new measure with some commonly used measures. The purpose is not to show which GAN is better but to show how the results (values) of our measure compares to those of existing measures.

3.1. One image type by DCGAN

Table 1. Measure values for different numbers of generated images

#	LS	IS	FID	r1NNC
120	0.613	1.435	148.527	0.850
240	0.644	1.424	134.484	0.858
480	0.636	1.409	135.317	0.821
960	0.622	1.447	145.142	0.833
1200	0.630	1.426	141.818	0.862
2400	0.628	1.431	146.109	0.850
4800	0.622	1.440	145.109	0.851

Dotted line: to the left are our proposed measures; to the right are compared measures.

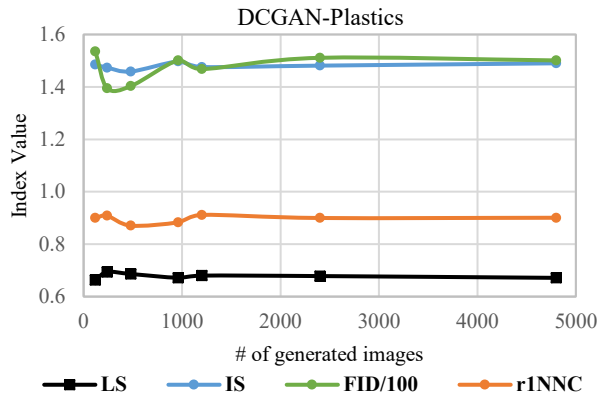


Fig. 3 Plots of values in Table 1.

To test the proposed measures, in the first experiment, we used one type of image (Plastics; 12 images) from the USPTex database [23] to train a DCGAN. Then, the trained GAN generated several groups containing different numbers of synthetic images. Finally, we compute our proposed measure, IS, FID and r1NNC results by using these generated images and 12 real images; the results are shown in Table 1.

Computations of **FID** and **r1NNC** require that the two image sets have the same number of images. We divided the generated images into many 12-image subsets to compute the indexes with 12 real images and then found their average values. Fig. 3 shows the plots of these indexes. FID is scaled by 0.01 to fit the axes. The result indicates that these indexes are stable to different numbers of testing images, especially when the number is greater than 1000.

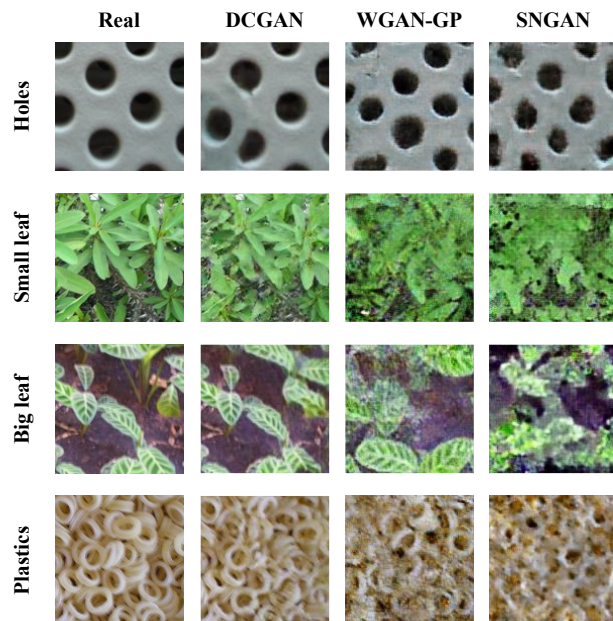


Fig. 4 Column 1: samples from 4 types' real image; column 2-4: samples from synthetic images of 3 GANs trained by the 4 types' images

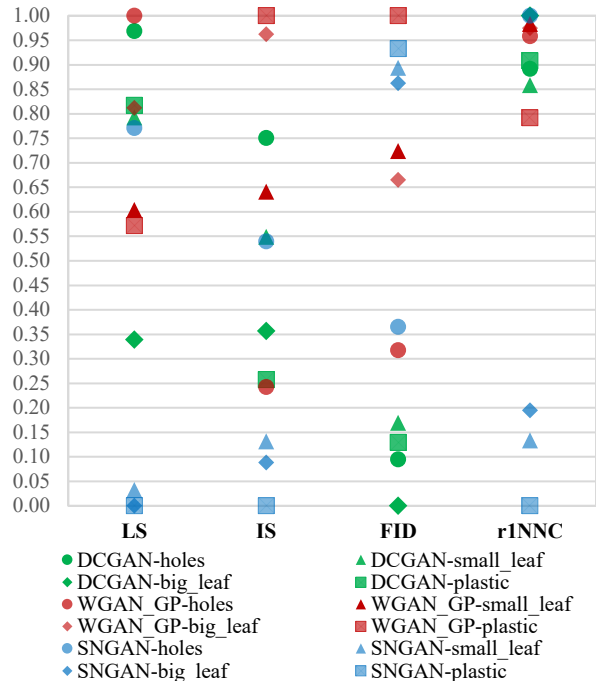


Fig. 5 Normalized indexes. X-axis shows indexes and y-axis shows their normalized values. Colors are for generators and shapes are for image types; see details in legend.

3.2. Four image types and three GANs

In the second experiment, four types of image (Holes, Small leaves, Big leaves, and Plastics; 12 images for each type) are used to train three GANs (DCGAN, WGAN-GP, and SNGAN). Then, the trained GANs generated 1,200 synthetic images for each type. Twelve sets of synthetic images were generated; Fig. 4 shows samples from 4 real image sets and 12 generated image sets. Visual examination of these synthetic images indicates that the DCGAN seems to give the most images similar to the real ones, but many of its generated images are duplications of real ones. Thus, the DCGAN overfitted the training data. The SNGAN's generated images are most dissimilar from real images; they lack the inheritance feature. The WGAN-GP well balanced the creativity and inheritance features.

Finally, we applied these measures on the 12 generated image sets; results are shown in Table 2. Fig. 5 shows plots of results. To emphasize the order of each index for different generators and image type, values are normalized from 0 to 1 by columns for plotting. Table 3 averaged scores by GANs. To compare the three GANs, Table 3 shows summarized results and Fig. 5 gives more details. For the best generator, the proposed LS index agrees with IS, 1NNC, and the visual appearance of generated images. Since the DCGAN overfitted to training data, it lacks creativity, but FID ranks it as the best model, and FID ranks SNGAN as the

worst because it may lack diversity. At this point, FID agrees with LS, IS, and 1NNC.

Table 2. Measure results

*	LS	IS	FID	r1NNC
DC- holes	0.747	1.222	102.805	0.892
DC-sl	0.611	1.171	155.973	0.858
DC-bl	0.262	1.321	172.296	1.000
DC- plastics	0.630	1.426	141.818	0.908
W- holes	0.771	1.163	233.277	0.958
W-sl	0.465	1.369	400.036	0.983
W-bl	0.626	1.536	375.987	0.975
W- plastics	0.441	1.555	513.268	0.792
SN- holes	0.594	1.317	252.857	1.000
SN-sl	0.025	1.105	469.795	0.133
SN-bl	0.000	1.083	456.813	0.195
SN- plastics	0.000	1.037	485.716	0.000

* Generator models: DC: DCGAN, W: WGAN-GP, SN: SNGAN. Generated image types: holes, sl: small leaves, bl: big leaves, plastics. Dotted line: to the left are our proposed measures; to the right are the compared measures.

Table 3. Measure results averaged by generators

GAN Model	LS	IS	FID [†]	r1NNC
DCGAN	0.562	1.285	143.223	0.915
WGAN-GP	0.576	1.406	380.642	0.927
SNGAN	<u>0.155</u>	<u>1.135</u>	<u>416.295</u>	<u>0.332</u>

Bold value: the best model by the measure of this column. Underline: the worst model by the measure of this column. Dotted line: to the left are our proposed measures; to the right are the compared measures. †FID: lower score is better.

3.3. Five GANs on CIFAR-10

Table 4. Measure results on CIFAR-10

GAN Model	LS	IS	FID [†]	r1NNC
DCGAN	0.833	4.311	147.110	0.772
WGAN-GP	0.957	3.408	136.121	0.932
SNGAN	<u>0.593</u>	<u>2.049</u>	<u>219.762</u>	<u>0.534</u>
LSGAN	0.745	3.405	136.132	0.716
SAGAN	0.688	2.075	206.046	0.545

Bold value: the best model by the measure of this column. Underline: the worst model by the measure of this column. Dotted line: to the left are our proposed measures; to the right are the compared measures. †FID: lower score is better.

In the third experiment, we used the CIFAR-10 dataset that is widely used in machine learning to train more types of GANs (DCGAN, WGAN-GP, SNGAN, LSGAN, and SAGAN). A 2,000-image subset had been taken from the training set of CIFAR-10 to train the five GANs; it consists

of 10 classes. Then, each trained GAN generated 2,000 synthetic images and we applied the LS, IS, FID, and 1NNC measures to the five generated image sets. Results are shown in Table 4. LS agrees with FID and 1NNC that WGAN-GP is the best GAN model but IS ranks DCGAN as the best model. For the worst model, LS agrees with all the other measures.

3.4. Virtual GANs on MNIST

To emphasize the measurements of creativity, diversity, and inheritance, in the fourth experiment, we created five artificial image sets to simulate the optimal generated images and generated images that lack creativity, lack diversity, lack both creativity and diversity, and lack inheritance. Images are taken or modified from the MNIST database [24], which contains 28×28 -pixel handwritten-digit images with labels “0”, “1”, “2”, ..., “9”. Fig. 6 describes how the five artificial sets were built.

Three subsets containing 2,000, 2,000 and 20 images were randomly selected from handwritten digit “8” images in MNIST. There is no common image in the three sets. One set having 2,000 images was considered as the **optimal generated set** because these images come from the same source of real data. The **lack-of-diversity set** was generated by repeatedly copying the 20 images 100 times. Another 2,000-image set was considered as the **real set** and used to generate the **lack-of-creativity set** by shifting all images with the median filter. Since filtering could slightly change images and keep their main information, each image after filtering is similar to its original version *i.e.* the shifted images lack creativity. Picking 20 images from the lack-of-creativity set and repeatedly copying them 100 times

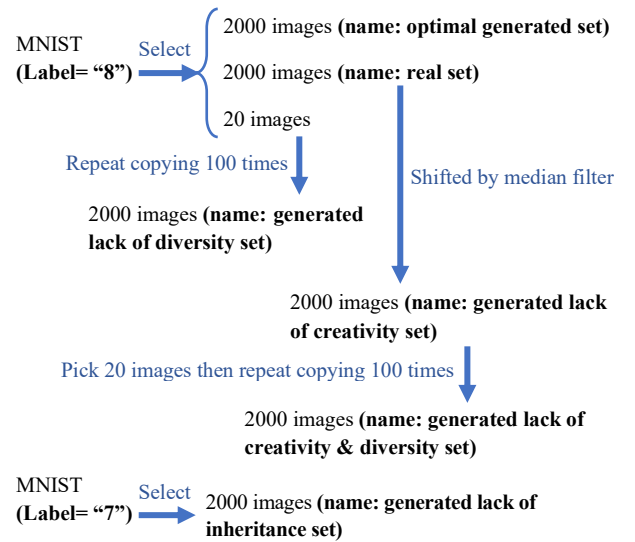


Fig. 6. Processes to build real set and generated sets including optimal generated images and generated images lack creativity, lack diversity, lack creativity & diversity, and lack inheritance.

generates the **lack-of-creativity & diversity set**. The **lack-of-inheritance set** contains 2,000 images randomly selected from handwritten digit “7” images in MNIST because the handwritten digit “7” is greatly different from digit “8”.

We considered that the real set is the training set to train five virtual GAN models. The optimal generated set as generated from an optimal GAN and the other four sets were generated from four different GANs having respective drawbacks. Then, we applied the LS, IS, FID and 1NNC measures to the five “generated” image sets. Results are shown in Table 6.

Table 5. Measure results from virtual GAN models

Virtual GAN Model	LS	IS	FID [†]	r1NNC
Optimal	0.994	1.591	4.006	0.978
Lack Creativity	0.820	2.112	67.310	0.039
Lack Diversity	0.892	<u>1.299</u>	59.112	<u>0.002</u>
Lack C & D*	0.775	1.418	116.656	0.775
Lack Inheritance	<u>0.526</u>	1.941	<u>130.827</u>	0.462

* C & D is creativity & diversity. **Bold value**: the best model by the measure of this column. Underline: the worst model by the measure of this column. Dotted line: to the left are our proposed measures; to the right are the compared measures. †FID: lower score is better.

In this experiment, we know which GAN is the best one. Hence, we could state the concrete conclusion that LS, FID, and 1NNC successfully discover the best GAN model. As we discussed in Sec.1.2, results of IS confirm that it is not good at evaluating the creativity and inheritance of GANs because it gives them higher scores (2.112 and 1.941) than the best case (1.591), and IS is prone to require the diversity. Other measures also show their characteristics: LS agrees with FID that the worst model is lack of inheritance, 1NNC indicates that the model lacking diversity is the worst, and

thus 1NNC values diversity as IS does. By contrast, LS and FID value creativity more among diversity and creativity.

4. Discussion

Since Geirhos et al., 2019 [25] recently reported that CNNs trained by ImageNet have a strong bias to recognize textures rather than shapes, we chose texture images to train GANs. From results in Table 3, the proposed LS agrees with IS and 1NNC that the WGAN-DP performs the best and SNGAN performs the worst on selected texture images. As shown in Table 4, LS makes the same evaluation on CIFAR-10 dataset. As shown in Fig. 5, SNGAN and WGAN-GP generate synthetic images that look different from real samples but SNGAN tends to generate very similar images; its diversity score is low. Hence, all measures rate SNGAN as performing worst on texture datasets. Results on CIFAR-10 dataset (Table 4) show a similar conclusion.

4.1. Evaluation of GAN measures

Results in Table 3 and Table 4 indicate that LS is a promising measure for GAN; without a gold standard, however, it is difficult to compare GAN evaluation methods and to state which method is better when they performed similarly. To show measures’ characteristics and evaluate them in terms of the three respects of an ideal GAN, we artificially created five datasets (Fig. 6) as if they were generated from five virtual GANs trained on MNIST. In this controlled circumstance (Table 5), LS, FID, and 1NNC discerned the best GAN model. In addition, by analyzing the distributions of ICD and BCD sets, LS could provide evidence for the lack of creativity, diversity, and inheritance to explain its results. As with Fig. 2, we plot data and histograms of their ICD and BCD sets in Fig. 7 to show their

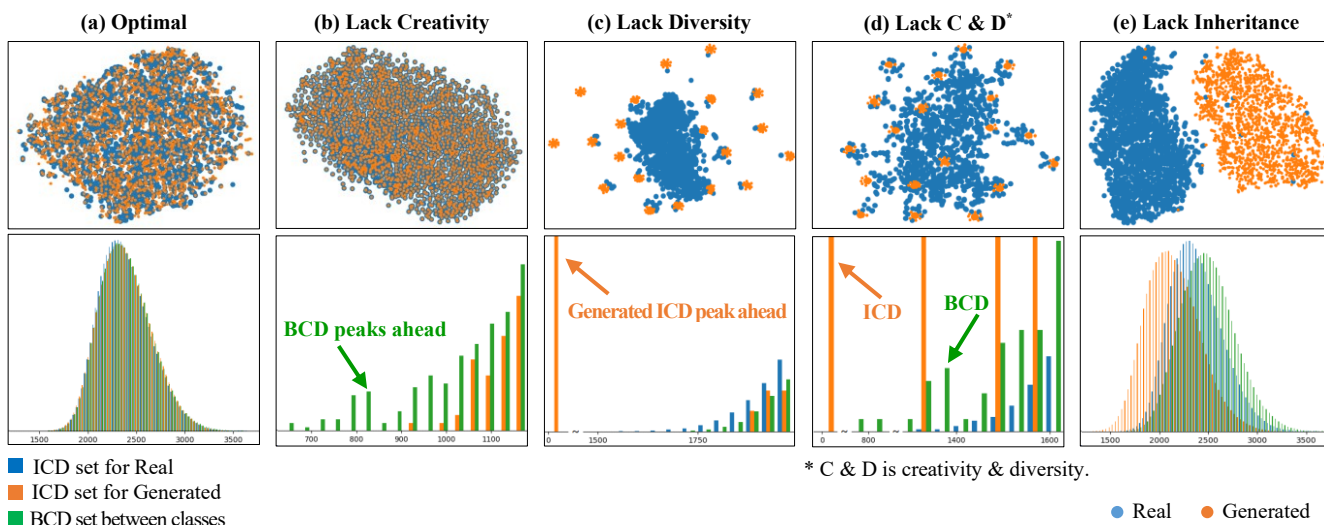


Fig. 7. Real and generated datasets from virtual GANs on MNIST. First row: the 2D tSNE plots of real (blue) and generated (orange) data points from each virtual GAN. Second row: histograms of ICDs (blue for real data; orange for generated data) and BCD for real and generated datasets. The histograms in (b)-(d) are zoomed to the beginning of plots; (a) and (e) have the entire histograms.

relationships with the LS. Each image in MNIST has 784 pixels so that these data are in a 784-dimensional space. To visually represent the data in two dimensions, we applied, the t-distributed Stochastic Neighbor Embedding (tSNE) [26] method. In contrast, the ICD and BCD sets were computed in the 784-dimensional space directly, without using any dimensionality reduction or embedding method.

As shown in Fig. 7, the ICD and BCD sets for computing the LS offer an interpretation of how LS works and verify that LS is able to detect the lack of creativity, diversity, and inheritance for GAN generated data, as we discussed in Sec. 2.2. Fig. 7(a) shows the real (training) data and data generated by the ideal GAN. Since distributions of the three sets are nearly the same, LS gets the highest score (close to 1, in Table 5). Fig. 7(b) shows the GAN lacks creativity. Almost every generated data point is overlapped with (or very close to) a real data point. Hence, the BCD set has some peaks at the beginning of plot. Lack of diversity is shown by Fig. 7(c). Most generated data points are not close to real data points, but some points are very close to each other. That results in a peak at the beginning of generated ICD plot. Any difference of the histograms of ICD and BCD sets will decrease the LS. Therefore, LS is affected by the isolated peaks of one distance set. Fig. 7(d) shows the combined effect. Generated data points are close to real data points and cluster in a few places. Both BCD and generated ICD peaks can be found at the beginning of plot. For the last Fig. 7(e), lack of inheritance means generated data are dissimilar from real data. The two kinds of data are distributed separately so that distributions of the three sets are all different, contrary to Fig. 7(a); that leads to the lowest LS.

4.2. Time complexity

Table 6. Time cost of measures

Measure*	LS	IS†	FID	INNC
CPU-Time (s)	106.087	295.158	574.285	274.245
GPU-Time (s)	-	68.471	180.435	-

* To test time costs, we used 2,000 real and 2,000 generated images from DCGAN on CIFAR-10 dataset. † IS only used the 2,000 generated images.

Both LS and INNC use the direct image comparison which is the Euclidean (l^2 -norm) distance between two images. The main time-cost of LS is to calculate ICD and BCD sets. LS’s time complexity for N (Class 1) and M (Class 2) data is about $O(N^2/2 + M^2/2 + MN)$. Although INNC also uses Euclidean distance between two images, its time complexity is about $O((M + N)^2)$; it is double the cost of LS. IS and FID use the Inception network to process images so that their time costs are greater than LS if running on our CPU (i7-6900K). As Table 6 shows, in one experiment, LS is computed faster than other measures. Running on GPU (GTX 1080 Ti) could accelerate the processing of neural networks, however, LS is still faster than FID; and, IS processes only half the number of images.

Moreover, LS also could be accelerated by moving it to run on a GPU in the future. In conclusion, LS has superior performance in terms of time complexity.

4.3. Contributions and future works

The commonly used GAN measures like IS, FID and INNC have drawbacks. As noted above, IS depends on the Inception network trained by ImageNet and IS lacks the ability to detect overfitting (creativity) and inheritance. FID also depends on the pre-trained Inception network and a Gaussian distribution assumption of feature vectors from the network. INNC requires that the number of real data be equal to the number of generated data, and the local conditions of distributions will greatly influence its result because of its use of the 1-nearest neighbor. The proposed LS is designed to avoid those disadvantages. We have created three criteria (creativity, diversity, and inheritance) to describe ideal GANs. And we have shown that LS evaluates a GAN by examining the three aspects in a uniform framework. In addition, LS does not need a pre-trained classifier, image analysis methods, nor *a priori* knowledge of distributions.

LS uses a very simple process -- it calculates only Euclidean distances and then applies the K-S test; those methods are independent of image types, numbers, and sizes. In particular, the LS offers a distinctly new way to measure the separability of real and generated data. Besides evaluation of GANs, LS could measure data complexity as well. The proposed novel model-independent measure for GAN evaluation has clear advantages in theory and is demonstrated to be worthwhile for future GAN studies.

Results also show that a GAN that performs well with one type of image may not be do so with other types. For example, in Table 2 and Fig. 5, we see that when measured by LS, IS, FID and INNC, the SNGAN performs much better on Holes images than on other types. Hence, in future works, we will examine the proposed measures on more types of images and GAN models.

5. Conclusion

The novel GAN measure -- LS -- we propose here can directly analyze the generated images without using a pre-trained classifier and it is stable with respect to the number of images. The strength of our method is that it avoids the disadvantages of existing methods, such as IS, FID, and INNC, and has fewer constraints and wider applications.

Furthermore, LS could evaluate the performance of GANs well and provide explanation of results in the three main respects of optimal GANs according to our expectations of ideal generated images. Such explanations help us to deepen our understanding of GANs and of other GAN measures that will help to improve GAN performance.

References

- [1] I. Goodfellow *et al.*, “Generative Adversarial Nets,” in *Advances in Neural Information Processing Systems 27*, Z. Ghahramani, M. Welling, C. Cortes, N. D. Lawrence, and K. Q. Weinberger, Eds. Curran Associates, Inc., 2014, pp. 2672–2680.
- [2] Y. Hong, U. Hwang, J. Yoo, and S. Yoon, “How Generative Adversarial Networks and Their Variants Work: An Overview,” *ACM Comput. Surv.*, vol. 52, no. 1, pp. 1–43, Feb. 2019, doi: 10.1145/3301282.
- [3] A. Hindupur, *the-gan-zoo: A list of all named GANs!* 2018.
- [4] C. Wang, C. Xu, C. Wang, and D. Tao, “Perceptual Adversarial Networks for Image-to-Image Transformation,” *IEEE Trans. Image Process.*, vol. 27, no. 8, pp. 4066–4079, Aug. 2018, doi: 10.1109/TIP.2018.2836316.
- [5] Z. Yi, H. Zhang, P. Tan, and M. Gong, “DualGAN: Unsupervised Dual Learning for Image-to-Image Translation,” in *2017 IEEE International Conference on Computer Vision (ICCV)*, Venice, Oct. 2017, pp. 2868–2876, doi: 10.1109/ICCV.2017.310.
- [6] J. Li, X. Liang, Y. Wei, T. Xu, J. Feng, and S. Yan, “Perceptual Generative Adversarial Networks for Small Object Detection,” in *2017 IEEE Conference on Computer Vision and Pattern Recognition (CVPR)*, Honolulu, HI, Jul. 2017, pp. 1951–1959, doi: 10.1109/CVPR.2017.211.
- [7] C. Ledig *et al.*, “Photo-Realistic Single Image Super-Resolution Using a Generative Adversarial Network,” in *2017 IEEE Conference on Computer Vision and Pattern Recognition (CVPR)*, Honolulu, HI, Jul. 2017, pp. 105–114, doi: 10.1109/CVPR.2017.19.
- [8] Z. Pan, W. Yu, X. Yi, A. Khan, F. Yuan, and Y. Zheng, “Recent Progress on Generative Adversarial Networks (GANs): A Survey,” *IEEE Access*, vol. 7, pp. 36322–36333, 2019, doi: 10.1109/ACCESS.2019.2905015.
- [9] H. Wu, S. Zheng, J. Zhang, and K. Huang, “GP-GAN: Towards Realistic High-Resolution Image Blending,” in *Proceedings of the 27th ACM International Conference on Multimedia - MM '19*, Nice, France, 2019, pp. 2487–2495, doi: 10.1145/3343031.3350944.
- [10] A. Borji, “Pros and cons of GAN evaluation measures,” *Comput. Vis. Image Underst.*, vol. 179, pp. 41–65, Feb. 2019, doi: 10.1016/j.cviu.2018.10.009.
- [11] T. Salimans *et al.*, “Improved Techniques for Training GANs,” in *Advances in Neural Information Processing Systems 29*, D. D. Lee, M. Sugiyama, U. V. Luxburg, I. Guyon, and R. Garnett, Eds. Curran Associates, Inc., 2016, pp. 2234–2242.
- [12] M. Heusel, H. Ramsauer, T. Unterthiner, B. Nessler, and S. Hochreiter, “GANs Trained by a Two Time-Scale Update Rule Converge to a Local Nash Equilibrium,” in *Advances in Neural Information Processing Systems 30*, I. Guyon, U. V. Luxburg, S. Bengio, H. Wallach, R. Fergus, S. Vishwanathan, and R. Garnett, Eds. Curran Associates, Inc., 2017, pp. 6626–6637.
- [13] D. Lopez-Paz and M. Oquab, “Revisiting Classifier Two-Sample Tests,” in *International Conference on Learning Representations*, 2017, [Online]. Available: <https://openreview.net/forum?id=SJKXfE5xx>.
- [14] A. Radford, L. Metz, and S. Chintala, “Unsupervised Representation Learning with Deep Convolutional Generative Adversarial Networks,” in *International Conference on Learning Representations*, 2016, [Online]. Available: <http://arxiv.org/abs/1511.06434>.
- [15] I. Gulrajani, F. Ahmed, M. Arjovsky, V. Dumoulin, and A. C. Courville, “Improved Training of Wasserstein GANs,” in *Advances in Neural Information Processing Systems 30*, I. Guyon, U. V. Luxburg, S. Bengio, H. Wallach, R. Fergus, S. Vishwanathan, and R. Garnett, Eds. Curran Associates, Inc., 2017, pp. 5767–5777.
- [16] T. Miyato, T. Kataoka, M. Koyama, and Y. Yoshida, “Spectral Normalization for Generative Adversarial Networks,” in *International Conference on Learning Representations*, 2018, [Online]. Available: <https://openreview.net/forum?id=B1QRgzIT->.
- [17] X. Mao, Q. Li, H. Xie, R. Y. K. Lau, Z. Wang, and S. P. Smolley, “Least Squares Generative Adversarial Networks,” in *2017 IEEE International Conference on Computer Vision (ICCV)*, Oct. 2017, pp. 2813–2821, doi: 10.1109/ICCV.2017.304.
- [18] H. Zhang, I. Goodfellow, D. Metaxas, and A. Odena, “Self-Attention Generative Adversarial Networks,” in *International Conference on Machine Learning*, May 2019, pp. 7354–7363, Accessed: May 22, 2020. [Online]. Available: <http://proceedings.mlr.press/v97/zhang19d.html>.
- [19] C. Szegedy, V. Vanhoucke, S. Ioffe, J. Shlens, and Z. Wojna, “Rethinking the Inception Architecture for Computer Vision,” in *2016 IEEE Conference on Computer Vision and Pattern Recognition (CVPR)*, Las Vegas, NV, USA, Jun. 2016, pp. 2818–2826, doi: 10.1109/CVPR.2016.308.
- [20] J. Deng, W. Dong, R. Socher, L.-J. Li, Kai Li, and Li Fei-Fei, “ImageNet: A large-scale hierarchical image database,” in *2009 IEEE Conference on Computer Vision and Pattern Recognition*, Jun. 2009, pp. 248–255, doi: 10.1109/CVPR.2009.5206848.
- [21] S. Kullback and R. A. Leibler, “On Information and Sufficiency,” *Ann. Math. Stat.*, vol. 22, no. 1, pp. 79–86, 1951.
- [22] “scipy.stats.kstest — SciPy v0.14.0 Reference Guide.” <https://docs.scipy.org/doc/scipy-0.14.0/reference/generated/scipy.stats.kstest.html> (accessed Nov. 06, 2019).
- [23] A. R. Backes, D. Casanova, and O. M. Bruno, “Color texture analysis based on fractal descriptors,” *Pattern Recognit.*, vol. 45, no. 5, pp. 1984–1992, May 2012, doi: 10.1016/j.patcog.2011.11.009.
- [24] Y. LeCun, C. Cortes, and C. J. Burges, “MNIST handwritten digit database,” 2010.
- [25] R. Geirhos, P. Rubisch, C. Michaelis, M. Bethge, F. A. Wichmann, and W. Brendel, “ImageNet-trained CNNs are biased towards texture; increasing shape bias improves accuracy and robustness,” *ArXiv181112231 Cs Q-Bio Stat*, Jan. 2019, Accessed: Feb. 03, 2020. [Online]. Available: <http://arxiv.org/abs/1811.12231>.
- [26] L. van der Maaten and G. Hinton, “Visualizing Data using t-SNE,” *J. Mach. Learn. Res.*, vol. 9, no. Nov, pp. 2579–2605, 2008.